

# Hydrothermal growth of well-aligned ZnO nanorod arrays: Dependence of morphology and alignment ordering upon preparing conditions

Min Guo<sup>a,b,\*</sup>, Peng Diao<sup>c</sup>, Shengmin Cai<sup>b</sup>

<sup>a</sup>Department of Physical Chemistry, University of Science and Technology Beijing, Beijing 100083, PR China

<sup>b</sup>College of Chemistry and Molecular Engineering, Peking University, Beijing 100871, PR China

<sup>c</sup>School of Materials Science and Engineering, Beijing University of Aeronautics and Astronautics, Beijing 100083, PR China

Received 3 December 2004; received in revised form 20 March 2005; accepted 21 March 2005

Available online 21 April 2005

## Abstract

Well-aligned ZnO nanorod arrays were prepared on substrates by hydrothermal growth under different conditions. The effect of preparing conditions on the deposition of ZnO nanorods was systematically studied by scanning electron microscopy, X-ray diffraction and photoluminescence spectroscopy. It is demonstrated that the growth conditions such as pre-treatment of the substrates, growth temperature, deposition time and the concentration of the precursors have great influence on the morphology and the alignment ordering of ZnO nanorod arrays. Pre-treatment of substrates, including dispersion of ZnO nanoparticles and subsequent annealing, not only plays a main role in governing the rod diameter, but also greatly improves the rod orientation. Although the rod diameter and its distribution are mainly determined by pre-coated ZnO nanoparticles, they can also be monitored to some extent by changing the concentration of the precursors. The growth temperature has a little influence on the orientation of nanorods but it has great impact on their aspect ratio and the photoluminescent property. Kinetic studies show that the growth of ZnO nanorods contains two distinct step: a fast steps within the first hour, in which the nanorods tend to be short and wide, and a slow step, in which long rods with high aspect ratio are obtained.

© 2005 Elsevier Inc. All rights reserved.

**Keywords:** Hydrothermal deposition; Zinc oxide; Well-aligned nanorod arrays

## 1. Introduction

Nanoscale one-dimensional (1D) semiconductor materials have attracted great research interest because of their importance both in fundamental research and in technological applications [1]. Considerable efforts have been devoted to the synthesis of 1D nanostructure, and various approaches have been demonstrated for the fabrication of semiconducting nanowire or nanorods [2]. To date, although many research efforts are still directed

toward synthesizing randomly oriented 1D semiconductor materials, it has been realized that the construction of semiconductor nanostructures, with well-ordered alignment and morphology, is critical for scientific and technological applications [3,4].

ZnO, as a wide band-gap semiconductor, has been widely investigated due to its promising application in catalysis [5], Grätzel-type solar cells [6], short-wavelength light-emitting devices [7,8], transparent conductor [9], chemical sensors [10] and piezoelectric materials [11]. A recent report of ultraviolet (UV) lasing action from well-aligned ZnO nanorod arrays [12] has greatly stimulated interest in synthesizing ZnO-based nanostructures, which were composed of well-aligned ZnO nanowires or nanorods. Several approaches, including

\*Corresponding author. Department of Physical Chemistry, University of Science and Technology Beijing, Beijing 100083, PR China. Fax: +86 10 6233 3477.

E-mail address: [guomin@metall.ustb.edu.cn](mailto:guomin@metall.ustb.edu.cn) (M. Guo).

vapor–liquid–solid (VLS) growth [12], chemical vapor deposition (CVD) [13,14], electrochemical deposition (ED) [15] and hydrothermal approaches [16–19], have been developed for fabricating well-aligned 1D ZnO nanostructures. Compared to VLS, CVD and ED methods that require sophisticated equipment and rigorous conditions such as single-crystalline substrates [12–15] and relatively high temperature ( $\geq 890^\circ\text{C}$  for VLS [12] and  $500^\circ\text{C}$  for CVD [13]), the hydrothermal routes are more convenient and economic for large-scale preparation of well-ordered ZnO nanowire/nanorod arrays.

Based on the principle that heteronucleation onto a substrate occurs more easily at a certain saturation ratio than in homogeneous solution, Vayssieres et al. [20,21] reported the preparation of highly oriented ZnO microrods and microtubes via a simple low-temperature hydrothermal method. Recently, by decreasing the overall concentration of the reagents, while keeping the  $\text{Zn}^{2+}$  to amine ratio constant as 1:1, they have successfully reduced the diameter of the ZnO rod from 1–2  $\mu\text{m}$  to 100–200 nm [17]. Boyle et al. [22] developed a two-step approach, which involves a pre-coating step of ZnO template layer and a subsequent solution deposition process, to produce perpendicularly oriented ZnO submicrorods. Recently, Govender et al. [16] synthesized well-oriented ZnO nanocolumns on Au-coated  $\text{SnO}_2$  substrates via hydrothermal route, and observed room-temperature lasing from the nanocolumn arrays. This finding indicates that ZnO nanorod arrays grown from solution are suitable for UV laser construction. Imai and Yamabi [18] studied the essential conditions for the growth of wurtzite ZnO films in aqueous solution by changing pH and complex agent, and also obtained arrayed ZnO nanorods on modified substrates. Very recently, Greene et al. [19] reported the formation of ZnO nanorod arrays on different substrates and studied their photoluminescent properties as a function of temperature.

Even though the hydrothermal approaches are simple, economic and suitable for large-scale production, the quality of the arrayed ZnO nanorods fabricated using these methods are not as good as that of nanorods prepared via VLS, CVD and ED methods. For example, the X-ray diffraction (XRD) patterns of ZnO nanorod arrays grown by VLS [12], CVD [13,14] and ED [15] show only the diffraction peaks of 002 and 004, indicating that all the nanorods are exactly perpendicularly oriented to the substrates. Whereas for ZnO nanorod arrays grown by hydrothermal routes, other diffraction peaks such as 100, 101, 102, etc. were also observed [16,17], suggesting that part of the nanorods deviated from the substrate normal. Furthermore, the diameter distribution of ZnO nanorods grown from solution is wider than that of nanorods prepared by VLS and CVD methods. As a result, controlling the

orientation, morphology, growth density, diameter distribution and aspect ratio of arrayed ZnO nanorods/nanowires is still the most challenging issue in hydrothermal deposition of well-aligned ZnO nanorod/nanowire arrays. However, detailed studies on these issues up to now are inadequate. So, it is necessary to explore systematically the effect of preparing conditions on the growth of well-aligned ZnO nanorods in solution.

In this paper, we describe the hydrothermal growth of ZnO nanorod arrays under various conditions. We demonstrate that the preparing conditions such as the pre-treatment of substrates, deposition temperature, growth time and the concentration of the precursors have a great influence on the morphological features and the alignment ordering of ZnO nanorod arrays. We also show that the orientation, morphology, growth density, diameter and its distribution of the arrayed ZnO nanorods can be effectively controlled by using suitable preparing conditions.

## 2. Experimental section

### 2.1. Materials

All chemicals (Beijing Chemicals Co. Ltd.) were of analytical reagent grade and used without further purification. All the aqueous solutions were prepared using double distilled and ion-exchanged water. Indium tin oxide (ITO,  $10\ \Omega/\text{cm}^2$ ) glass plates were used as substrates and were cleaned by standard procedures prior to use.

### 2.2. Pre-treatment of the substrates

Two different methods were used to pre-treat the substrates.

- (A) *Precipitate pre-treating method.* Aqueous solutions of  $\text{Zn}(\text{NO}_3)_2$  (1 mL, 0.5 M) and methenamine (1 mL, 0.5 M) were added dropwise to  $1.5 \times 3.0\ \text{cm}^2$  ITO substrates. After 5 min deposition at room temperature and subsequent spin coating, the substrates were dried and then annealed at  $300^\circ\text{C}$  for 10 min. The resulting substrates are referred to as precipitate pre-treated substrates (PPT-substrates) in this paper.
- (B) *Colloid pre-treating method.* The preparation of the colloid solution for coating substrates was described elsewhere [23]. In detail, zinc acetate dihydrate ( $\text{Zn}(\text{CH}_3\text{COO})_2 \cdot 2\text{H}_2\text{O}$ ) was dissolved in the mixed solution of ethanolamine ( $\text{NH}_2\text{CH}_2\text{CH}_2\text{OH}$ ) and 2-methoxyethanol ( $\text{CH}_3\text{OCH}_2\text{CH}_2\text{OH}$ ). The concentrations of both  $\text{Zn}(\text{CH}_3\text{COO})_2$  and ethanolamine in the resulting solution are 0.75 M. The resulting mixture was then agitated at  $60^\circ\text{C}$  for

30 min to yield a homogeneous and stable colloid solution, which served as coating solution. The coating colloid solution ( $\sim 2$  mL) was dropped onto  $1.5 \times 3.0$  cm<sup>2</sup> ITO substrates for spin coating, then the substrates were dried and annealed at 300 °C for 10 min. The resulting substrates are referred to as colloid pre-treated substrates (CPT-substrates) in the following context.

### 2.3. Hydrothermal deposition

The precursor solutions were prepared by mixing Zn(NO<sub>3</sub>)<sub>2</sub> (0.1 M) with methenamine ((CH<sub>2</sub>)<sub>6</sub>N<sub>4</sub>, 0.1 M) while keeping their volume ratio at 1:1. For the experiments studying the effect of concentration, the volume ratio of the two solutions was kept constant at 1:1, while changing the concentrations to meet the experimental requirements. Unless specified, the hydrothermal growth was carried out at 95 °C in a quartz beaker placed in a sealed kettle by immersing the pre-modified or unmodified substrates in precursor solutions (60 mL).

### 2.4. Characterization

The morphology and size distribution of the nanorods were characterized using scanning electron microscopy (SEM) (Philips FEI XL30 SFEG operated at 5 or 10 KeV). XRD analysis was performed with a Rigaku Dmax-2000 diffractometer using CuK $\alpha$  radiation. Room-temperature photoluminescence (PL) spectra were recorded on a fluorescence spectrophotometer using Xe lamp with an excitation wavelength of 350 nm.

## 3. Results and discussion

### 3.1. Effects of substrate pre-treatment

#### 3.1.1. Effect of pre-coating layer of ZnO nanoparticles on ZnO nanorod growth

As is well known, the homogeneous nucleation of solid phase in solution usually does not occur even though the system is beyond the saturation concentration to some extent. The resistance to homogeneous nucleation is associated with the surface energy of forming a small nucleus. Although heterogeneous nucleation onto a foreign surface occurs more easily compared to homogeneous nucleation [20], the process is difficult to control due to the random and complex nature of the nucleus forming on a foreign surface. Therefore, from the aspect of heterogeneous nucleation, pre-coating the substrates with seeds of the same material as nanocrystals being grown is an effective

way to control the morphology, texture and even orientation of the deposited crystals.

Fig. 1 shows the SEM photographs of arrayed ZnO rods grown on substrates with or without pre-coated ZnO nanoparticle layers. From the top view and side view SEM images (Figs. 1b, c, e, f, h and i), it can be clearly seen that, no matter which pre-coating method was used, the obtained ZnO nanorod arrays have improved structure ordering. Figs. 1b, e and h clearly show that the average rod diameter decreases from microscale without substrate pre-treatment to nanoscale with substrate pre-treatment. Furthermore, with the pre-coating of ZnO nanoparticle layers, the diameter distribution of the rods becomes narrower and the rod density increases significantly. Side view SEM images (Fig. 1c, f and i) indicate that the length of the ZnO rod decreases after substrate pre-treatment. All these phenomena can be well explained by nucleation theories. For the growth of ZnO rods on unmodified ITO surface, the formation of initial ZnO nucleus is crucial. However, only a part of the initial nucleus, which occupies the most favorable energy sites and is beyond the critical nuclear size, can survive [24]. Consequently, the number of growing points on unmodified ITO substrates is limited and this leads to the slow consumption rate for precursors. As a result, the concentration of the precursor solution remains at a relatively high saturation level, and the crystal growth rate on each nucleus is greater compared to that on the substrate with a large number of nuclei. Moreover, early and newly presented ZnO nuclei will grow into larger and smaller rods, respectively. All this finally results in large diameter and length, wide diameter distribution and low growth density of the ZnO rods. As for ZnO rods grown on pre-modified substrates, large number of ZnO nanoparticles serve as crystal seeds, which promote the rate of relieving supersaturation, reduce the possibility of forming a new nucleus, lower the growth rate on single rod and, therefore, lead to small diameter, narrow diameter distribution, short length and high density of the ZnO rods.

Side view SEM images (Fig. 1c, f and i) also show that, before substrate pre-treatment, only a part of the ZnO rods align nearly normal to the substrate. However, after pre-treatment, the orientation of the rod is greatly improved. In order to provide further evidence that the improvement of the rod alignment is related to the introduction of ZnO nanoparticles onto substrates, we modified the substrates by the precipitate pre-treating method (see Section 2) with a very small amount of Zn(NO<sub>3</sub>)<sub>2</sub> and methenamine solutions (ca. 0.5 mL each). The substrates with a tiny drop of mixed solution were divided into two groups. Substrates in one group were immediately dried and heated at 300 °C for 10 min to produce ZnO nanoparticles. Substrates in another group were firstly rotated for a few minutes and

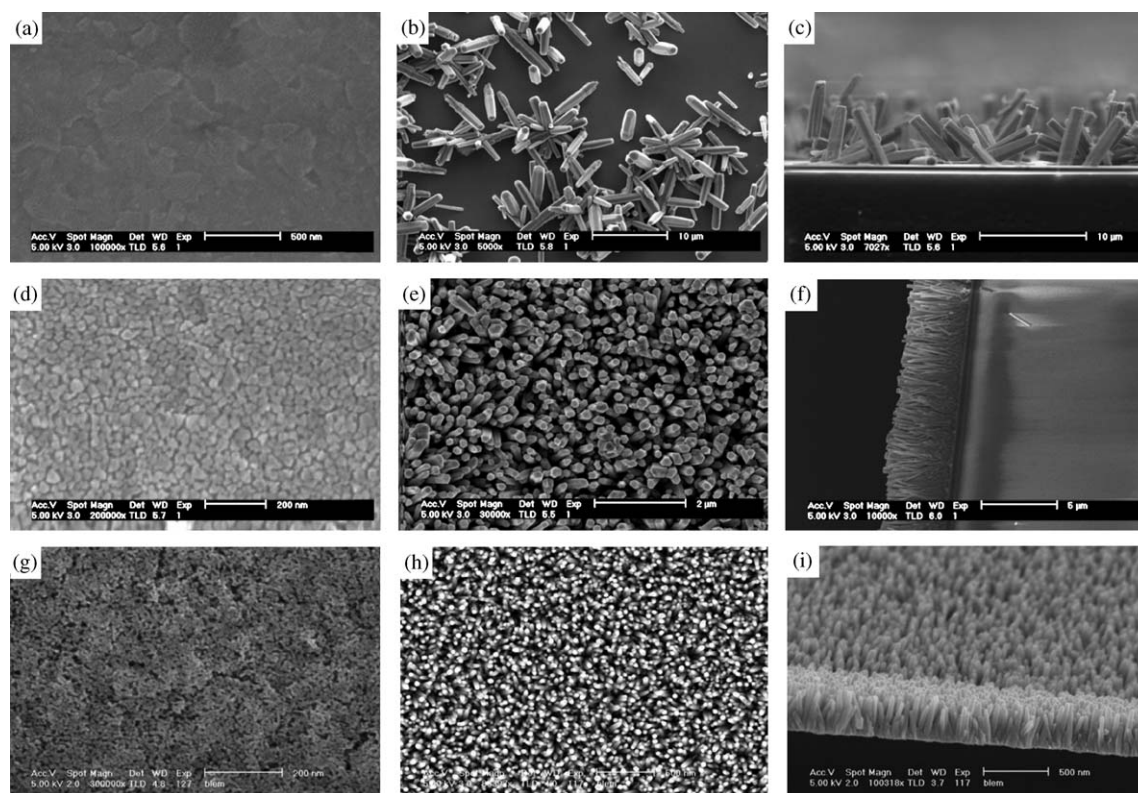


Fig. 1. SEM images of ZnO nanorods and corresponding substrates. (a) Unmodified ITO substrate, (b) top view, (c) side view of ZnO nanorods grown on unmodified substrate, (d) PPT-substrate, (e) top view, (f) side view of ZnO nanorods grown on PPT-substrate, (g) CPT-substrate, (h) top-view and (i) side view of ZnO nanorods grown on CPT-substrate. Growth time: 2 h.

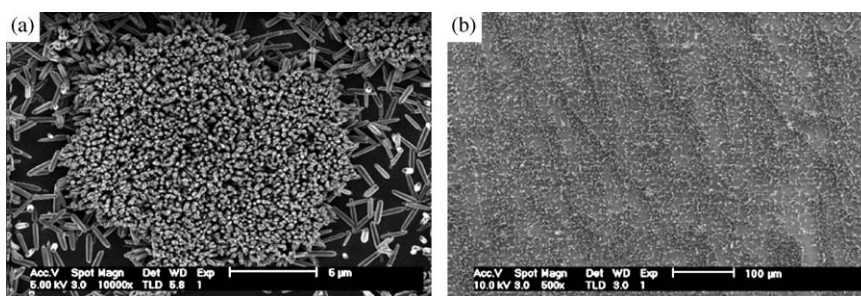


Fig. 2. Typical SEM images of the (a) patches and (b) lines of aligned ZnO nanorods showing the improvement of the nanorod alignment by pre-coated ZnO nanoparticles. Growth time: 2 h.

then dried and heated at 300 °C for 10 min. From the SEM image of all these substrates (not shown) patches of ZnO nanoparticles can be observed, and more interestingly, nanoparticle lines caused by centrifugal force can be seen on the rotated substrates. After hydrothermal growth, patches of well-aligned ZnO nanorods appear on both kinds of substrates, and as expected, standing nanorod lines can be clearly identified on the rotated substrates. Typical SEM images of the patch and lines of well-aligned nanorods are shown in Figs. 2a and b, respectively, which provide strong evidence that ZnO nanoparticles greatly promote the orientation of the nanorods. XRD spectra further

confirm the improvement of the alignment of ZnO rod arrays. Typical XRD patterns of ZnO rods deposited on modified and unmodified substrates are shown in Fig. 3 with all diffraction peaks well indexed to the standard diffraction pattern of hexagonal phase ZnO (Fig. 3d; JCPDS 36-1451), indicating a wurtzite structure with high crystallinity. In comparison with the standard XRD pattern, the much higher intensity of the 002 diffraction peaks for all samples indicates that ZnO rods are preferentially oriented perpendicularly to the substrate regardless of the pre-treatment. In addition, Figs. 3a, b and c show that the intensity ratio of 002 to 101 diffraction peaks increases significantly on

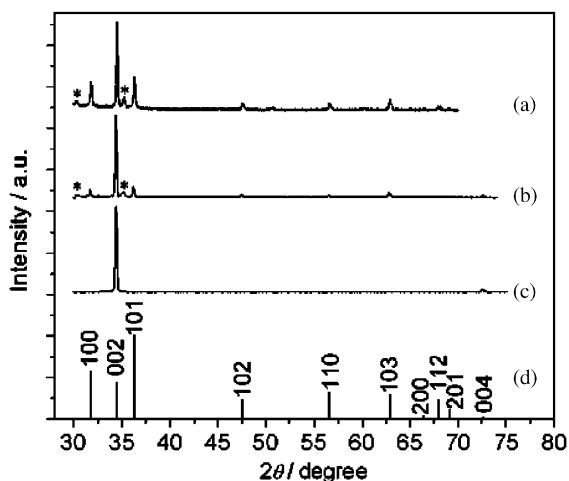


Fig. 3. XRD patterns of ZnO nanorods grown on: (a) unmodified ITO substrate (\*), (b) PPT-substrate, (c) CPT-substrate, and (d) standard ZnO (JCPDS No. 36-1451).

pre-treated substrates, suggesting that the orientation of ZnO rods is further improved. In other words, the introduction of ZnO nanoparticle layers on the substrate not only helps to control the rod density, diameter and its distribution, but also promotes the overall alignment ordering of ZnO rod arrays.

### 3.1.2. Effect of different pre-treating methods on ZnO nanorod growth

Although substrate pre-treatment leads to well-aligned ZnO nanorod arrays, ways of pre-treatment have a great influence on the morphology, texture and alignment of the rod arrays, as can be seen clearly from Figs. 1e, f, h and i. The diameter distributions of the ZnO nanorods grown both on PPT- and CPT-substrates (see Section 2) are illustrated in Fig. 4. From Fig. 4 it can be clearly seen that nanorods grown on CPT-substrates have not only a smaller average diameter (~30 nm) compared to those grown on PPT-substrates (~150 nm), but also a narrower size distribution. Moreover, the nanorod growth density on CPT-substrates is about  $2.0 \times 10^{12}$  rod/cm<sup>2</sup>, which is much higher than the value of  $2.0 \times 10^9$  rod/cm<sup>2</sup> on PPT-substrates. The different rod diameters and densities are believed to be due to the difference of nanoparticle size generated by the two pre-coating methods (see Figs. 1d and g). Small crystal seed finally results in small rod size and high growth density.

The orientation of the nanorods grown on both CPT- and PPT-substrates were analyzed using XRD spectra, as shown in Figs. 3b and c. From Fig. 3c we note that, for the nanorod arrays grown on CPT-substrates, only the diffraction peaks of 002 and 004 appear, indicating excellent overall *c*-axis alignment of these nanorod arrays over a large substrate area. It should be pointed out that the XRD spectra of arrayed ZnO

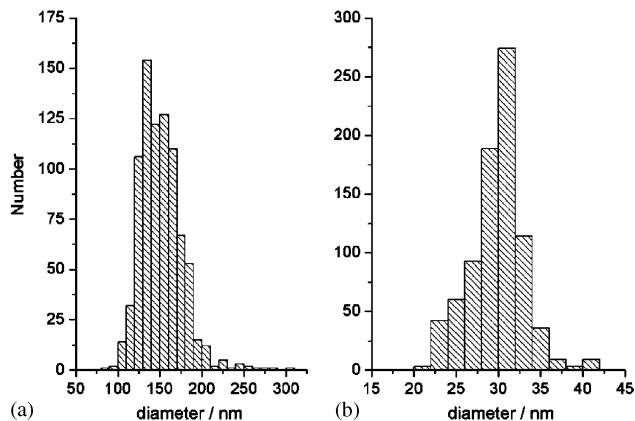


Fig. 4. Diameter distribution of ZnO nanorods grown on: (a) PPT-substrate and (b) CPT-substrate. Growth time: 2 h.

nanorods grown on CPT-substrates are quite different from those on PPT-substrates (Fig. 3b) and other substrates unmodified or pre-modified by other methods [16–18,20,22], wherein other diffraction peaks appear in addition to those of 002 and 004. This means that, by using a simple wet chemical approach, we can prepare high-ordering ZnO nanorod arrays, which were usually fabricated only by high-temperature methods [12–14].

### 3.1.3. Effect of substrate annealing on ZnO nanorod growth

In the process of preparing PPT- and CPT-substrates, there is a substrate annealing step that refers to heating the substrates, which are modified with coating solution and dried at room temperature. Herein, the annealing step in the preparation of CPT-substrates was taken, for example, to elucidate its effect on ZnO nanorod growth. Before annealing, the deposit layer, produced by drying the colloid solution of  $\text{Zn}(\text{CH}_3\text{COO})_2$  and  $\text{NH}_2(\text{CH}_2)_2\text{OH}$  on substrates, was composed of floc-like nanoparticles, as illustrated in Fig. 5a. These substrates will lead to, if used to grow ZnO nanorods without annealing, poor alignment of nanorod arrays (see Fig. 5b). Comparing Fig. 5a with Fig. 1g, we note that the relatively large floc-like particles change to small nanoparticles after annealing. The structural difference of the coating films before and after annealing was analyzed by XRD. From XRD spectra (Fig. 5c), no diffraction peaks of wurtzite ZnO can be observed before annealing. However, after annealing, 002, 100 and 101 diffraction peaks of wurtzite ZnO can be clearly identified with 002 peak having the highest intensity, indicating that the annealing treatment results in the formation of oriented ZnO nanoparticles on ITO substrates [25]. These oriented particles help form well-aligned ZnO nanorods in the hydrothermal process, as can be seen in Figs. 1h and i. Based on the above results, we believe that the difference of nanoparticle morphology and, more importantly, of the crystalline structure

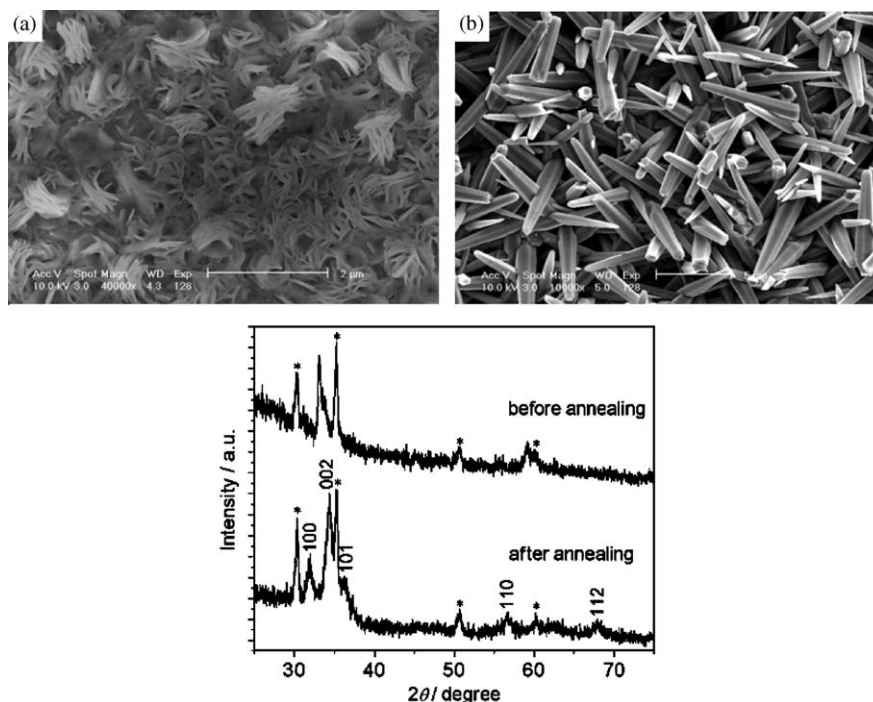


Fig. 5. SEM images of: (a) CPT-substrate dried in air but without annealing, (b) ZnO nanorods grown on this substrate, and (c) XRD pattern of CPT-substrate before and after annealing (\* peaks of ITO substrate). Growth time: 4 h.

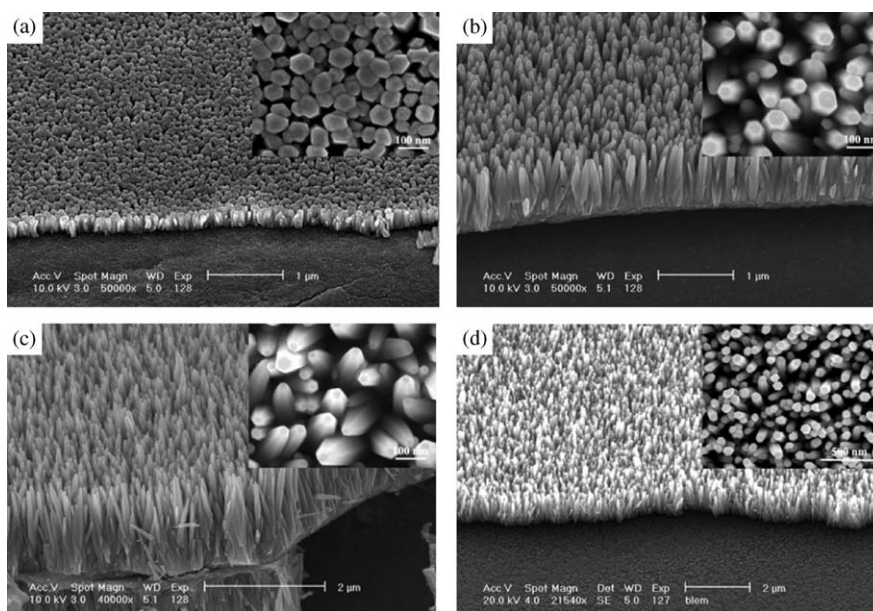


Fig. 6. SEM images of ZnO nanorods grown at: (a) 40 °C, (b) 60 °C (c) 80 °C and (d) 95 °C. Growth time: 4 h.

and the orientation of nanoparticles is responsible for the different alignment ordering of ZnO nanorod arrays.

### 3.2. Effect of temperature on ZnO nanorod growth

To study the effect of deposition temperature on the microstructure and properties of ZnO nanorod arrays, hydrothermal growth of the nanorod arrays were

performed on CPT-substrates at 40, 60, 80 and 95 °C, respectively. The corresponding SEM images of the nanorods grown at each temperature are shown in Fig. 6. From Fig. 6, we note that nearly all the ZnO nanorods are perpendicularly oriented to the substrate regardless of the growth temperature. Top-view SEM images (insets in Fig. 6) reveal that the nanorods are hexagonal, suggesting that the nanorods grow along the

[001] direction at various temperatures. XRD experiments of all samples give the same wurtzite ZnO pattern with 002 and 004 as the only appearing diffraction peaks, providing further evidence that the growth temperature has little influence on the orientation of the nanorods.

However, the growth temperature has a strong impact on the aspect ratio of the nanorods. As shown in Figs. 6(a)–(d), the average diameter of the nanorods remains almost unchanged but the average length of the nanorod increases greatly from ca. 200 nm to ca. 1.2  $\mu\text{m}$  when the deposition temperature is increased from 40 to 95  $^{\circ}\text{C}$ . This implies that the growth rate along [001] direction is more sensitive to temperature compared to those along [101] and [100] directions. Therefore, changing the growth temperature is one of the important means to control the aspect ratio of the nanorod arrays. Thin films composed of short ZnO nanocolumns are formed at low temperatures (for example, 40  $^{\circ}\text{C}$ ) due to the similar growth rates along all directions, while thick films composed of long nanorods are obtained at higher temperatures due to the greatly enhanced deposition rate along *c*-axis direction.

The UV and visible PL of ZnO nanocrystal is one of the most interesting and important property that has been intensively investigated recently. To study the influence of growth temperature on the optical property of the nanorod arrays, PL measurements were conducted at room temperature and the results are presented in Fig. 7. The PL spectra of ZnO nanorods prepared at different temperatures show the similar PL features, in which there are three obvious emission bands, including the strongest UV emission band centered at 387 nm, a weak blue band at around 470 nm, as well as a strong and broad green band at around 530 nm. The UV emission band results from the recombination of free exciton [26]. The green PL has been observed in ZnO nanocrystals grown by hydrothermal [27,28], VLS [26], CVD [13,14] and electrochemical methods [29,30], and its origin is commonly

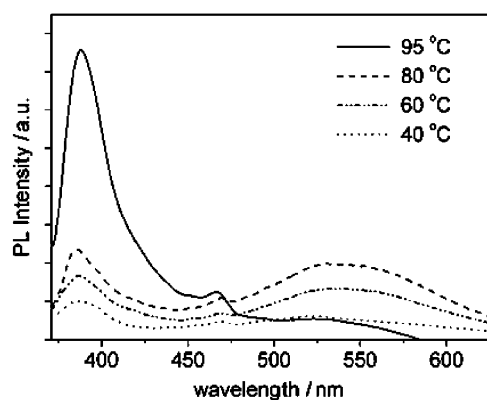


Fig. 7. Photoluminescence spectra of ZnO nanorods grown at: (a) 40  $^{\circ}\text{C}$ , (b) 60  $^{\circ}\text{C}$  (c) 80  $^{\circ}\text{C}$  and (d) 95  $^{\circ}\text{C}$ . Growth time: 4 h.

ascribed to the recombination of the photo-generated holes with the singly ionized oxygen vacancies [31]. More singly ionized oxygen vacancy defects will result in higher green PL intensity. The weak blue emission band was also observed in ZnO nanorod films fabricated by CVD method [13,14], but its mechanism is not fully understood.

Here, we should point out that the PL spectra in our case are quite different from those reported in Yong's work where a weak UV emission band at 378 nm and a very strong orange emission band at 605 nm were observed [19], though the preparation procedures for ZnO nanorod arrays in both works are similar except that we use higher precursor concentration, sealed reaction system and different substrate pre-treating method. The orange PL in Yang's work was also believed to be associated with the atomic defects in ZnO [19]. The green PL in our work and the orange PL in Yang's work imply that the preparing conditions have a great influence on the formation of different kinds of atomic defects in ZnO nanorods.

Fig. 7 also shows that the PL spectrum of ZnO nanorod arrays is dependent on the growth temperature. The band-edge PL intensity increases greatly and the green PL intensity decreases a lot when the growth temperature is increased to 95  $^{\circ}\text{C}$ . This means increasing the growth temperature to a certain extent will improve the crystal quality of ZnO nanorods. The reason for the growth temperature dependent PL, although not quite clear, is believed to be related to the formation mechanism of oxygen vacancies. Furthermore, for the nanorods grown at all temperatures in our case, the intensity ratio of band-edge PL to green PL is much larger compared to the ratio of band-edge PL to orange PL in Yang's work, suggesting that the ZnO nanorods prepared in our work have better crystal quality.

### 3.3. Effect of the concentration of precursors on ZnO nanorod growth

Vayssieres [20] reported the formation of ZnO microrods on unmodified substrates and found that the width of ZnO rods can be reduced from 1–2  $\mu\text{m}$  to 100–200 nm by lowering the overall concentration of the reactant while keeping the ratio of  $\text{Zn}^{2+}$  to amine constant at 1:1 [17]. Since the substrates used in our work were pre-modified with ZnO nanoparticles and the nanoparticles have a great influence on the diameter of the ZnO rods, it is necessary to investigate the effects of precursor concentration on the size of ZnO nanorods grown on modified substrates.

Fig. 8 shows the diameter distribution of ZnO nanorod arrays prepared on CPT-substrates in precursor solutions with different concentrations, from which it can be seen that the average diameter of the ZnO rod decreases from ca. 170 to 23 nm when the concentrations

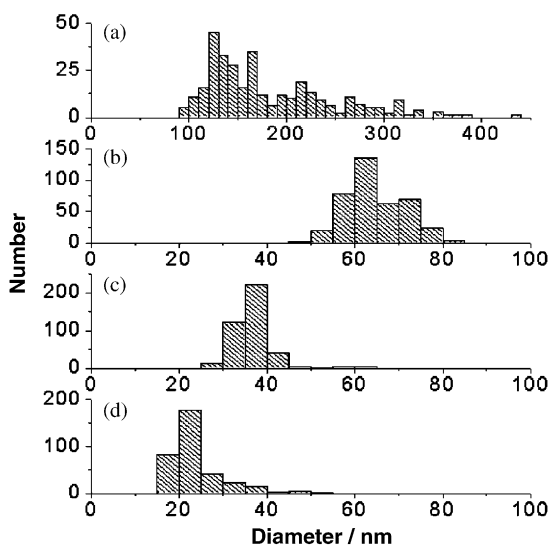


Fig. 8. Diameter distribution of ZnO nanorods grown at different reactant concentrations. The concentrations of both  $\text{Zn}(\text{NO}_3)_2$  and methenamine in mixed solution are: (a) 0.10 M, (b) 0.050 M, (c) 0.025 M and (d)  $2.5 \times 10^{-3}$  M. Growth time: 4 h.

of both  $\text{Zn}(\text{NO}_3)_2$  and methenamine are decreased from 0.10 to  $2.5 \times 10^{-3}$  M. The dependence of nanorod diameter on the concentration of reactant is not linear. At relatively high concentration range, the average rod diameter decreases nearly three times (from ca. 170 to 65 nm) when the concentration is lowered two times (from 0.10 to 0.050 M), but at low concentration range, the rod diameter decreases only a little (from ca. 38 to 23 nm) when the concentration is lowered an order of magnitude (from 0.025 to  $2.5 \times 10^{-3}$  M). It should be pointed out that, at low concentration range, the decreasing rate of rod width in our case is not as large as that reported in Vayssieres' work [17], where the nanorods were prepared on unmodified substrates and the rod width decreased the same order of magnitude as the concentration of reactant. This suggests that, for the ZnO nanorods prepared on modified substrates, the pre-coated ZnO nanoparticle layer plays the main role in governing the nanorod diameter, while on the other hand, the nanorod diameter can also be controlled to some extent by monitoring the concentration of the reactant. Furthermore, the diameter of the ZnO nanorod can also be reduced by decreasing the concentration of  $\text{Zn}(\text{NO}_3)_2$  while keeping that of methenamine constant.

From Fig. 8, it can also be seen that the diameter distribution of the nanorod becomes narrower with the decrease of reactant concentration. For the nanorods grown in 0.1 M precursor solution, the diameters of the ZnO nanorod distribute in a range from 90 to 390 nm (300 nm range width). When the concentration is reduced to 0.05 M, ca. 88% of the nanorods have diameters from 55 to 75 nm (20 nm range width). While the concentration is further reduced to  $2.5 \times 10^{-2}$  and

$2.5 \times 10^{-3}$  M, about 92% and 88% of the nanorods fall into the ranges from 30 to 45 nm (15 nm range width) and from 15 to 30 nm (15 nm range width), respectively. This fact suggests that well-aligned ZnO nanorods with uniform diameter can be fabricated at low concentrations. The low supersaturation degree is believed to be responsible for the small-diameter and the narrow size distribution of the ZnO nanorods grown in solutions with low concentration.

#### 3.4. Effect of growth time at early stage of solution deposition

Greene et al. [19] studied the average diameter and length of ZnO nanorods as a function of growth time, and reported a nearly linear dependence of these parameters on time. However, their work mainly focused on the long time growth. In fact, the early stage of hydrothermal growth, especially within the first 1 h, is very important for the ZnO nanorod arrays, because, at this stage, the supersaturation of the solution is the highest, and the nanocrystalline grains on which nanorods grow are generated with the help of pre-coated ZnO nanoparticles.

Kinetic studies of the nanorod growth were performed on PPT-substrates, since the nanorods grown on these substrates have a relatively larger diameter and length (see Section 3.1 B), which will make the observation easier, especially in the early stage of hydrothermal growth. Fig. 9 shows the SEM images of ZnO nanorod arrays grown on PPT-substrates within the first 1 h. A large amount of small hexagonal ZnO crystals can be narrowly identified when the growth time is 20 min (Fig. 9a); however, it is very hard to make out any hexagonal crystals when the growth time is less than 15 min. This implies that, within the first 20 min, the growth rate of nanorods is very low and the main process taking place in this initial stage might be the formation of hexagonal ZnO nanocrystalline grains on which the nanorods grow. After the initial 20 min, the growth of nanorods goes into a fast step and the hexagonal ends of nanorods can be clearly observed (Fig. 9b,c and d).

The dependence of the average diameter and length of nanorods on deposition time is illustrated in Fig. 10. For the growth in radial direction, two distinct growth kinetics can be observed: a very fast step, which takes less than an hour with a growth rate of  $\sim 2.4$  nm/min, by the end of which the average diameter reaches  $\sim 125$  nm, and a relatively slow step with a growth rate of  $\sim 0.54$  nm/min, which is about one-fourth of the rate in the fast step. In addition, results of long time deposition ( $> 6$  h) indicate that the average diameter almost stops to increase, and the nanorods begin to become rough, implying partially dissolving of the nanorods [20]. However, in the axial direction, the growth rate keeps



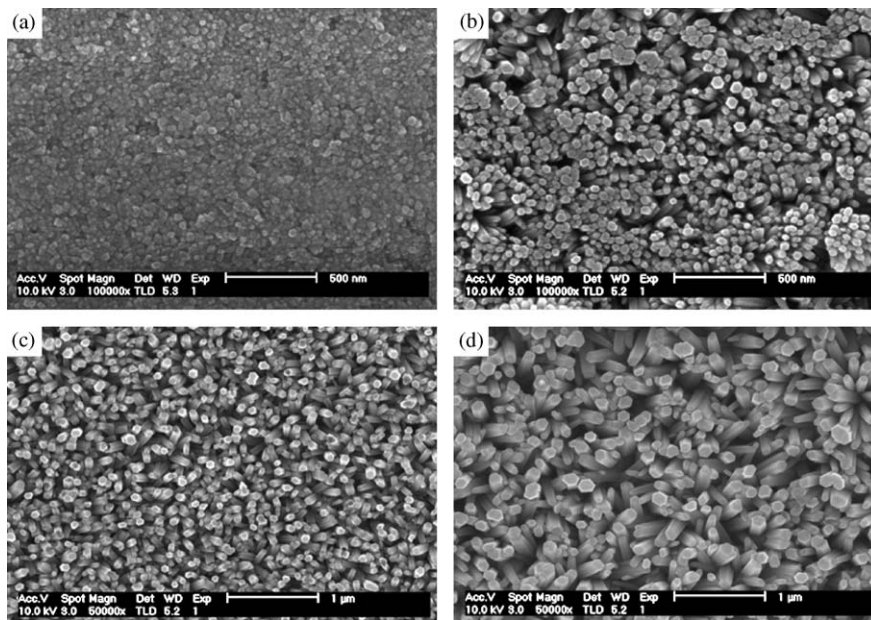


Fig. 9. SEM images of ZnO nanorods grown on PPT-substrates for: (a) 20 min, (b) 40 min, (c) 50 min and (d) 60 min.

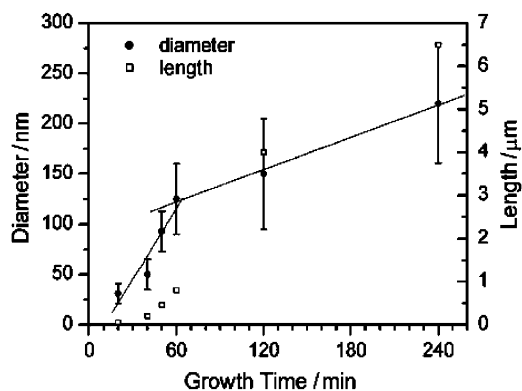


Fig. 10. Average diameter and length of ZnO nanorods as a function of growth time.

increasing within 2 h and only decreases slightly when the deposition time is beyond 2 h. All these results indicate that the early stage of hydrothermal deposition (within the first 1 h) benefits the growth in radial direction, in other words, ZnO nanorods with small aspect ratio tend to be formed in this stage. After the early stage, the radial growth rate drops abruptly while the axial growth rate still remains at a relatively high level, resulting in the long rods with high aspect ratio. Because the supersaturation of precursors is the highest in the early stage of deposition, it can also be deduced from Fig. 10 that high precursor concentration favors the formation of nanorods with larger average diameter. This is in good agreement with the effect of concentration on the rod diameter discussed in Section 3.3.

#### 4. Conclusions

In summary, to our knowledge, this work provides, for the first time, a systematic study of the hydrothermal growth of ZnO nanorod arrays on substrates. It has been demonstrated that the preparing conditions such as substrate's pre-treatment, deposition temperature, growth time and the concentration of the precursors have a great influence on the microstructure and ordering of ZnO nanorod arrays. The introduction of ZnO nanoparticle layer on substrate not only helps control the rod density, diameter and its distribution but also promotes the overall orientation of the nanorod arrays. The pre-coated ZnO nanoparticles with smaller size lead to small rod diameter, narrow diameter distribution and high growth density. The substrate annealing is crucial for the improvement of alignment ordering of ZnO nanorod arrays. Although growth temperature has little influence on the crystalline structure and the orientation of the nanorods, it has a great impact on the aspect ratio and the PL of the nanorods. High growth temperatures result in thick ZnO films composed of well-aligned nanorods with high aspect ratio. The concentration of precursors can influence the nanorod size to some extent, although the pre-coated ZnO nanoparticle layer plays the main role in governing the nanorod diameter. Kinetic studies show that the growth of ZnO nanorod in radial direction contains two distinct steps: a fast step in the early stage, in which short but wide rods are formed, and a slow step, in which long rods with high aspect ratio are obtained. Finally, this work sheds light on the

factors that govern the growth of well-aligned ZnO nanorod arrays, and gains access to the controlled fabrication of 1D alignments of other materials by hydrothermal deposition.

### Acknowledgments

Financial support from the National Natural Science Foundation of China (No. 20073003) is gratefully acknowledged.

### References

- [1] J. Hu, T.W. Odom, L.C.M. Ieber, *Acc. Chem. Res.* 32 (1999) 435–445.
- [2] Y. Xia, P. Yang, Y. Sun, Y. Wu, B. Mayers, B. Gates, Y. Yin, F. Kim, H. Yan, *Adv. Mater.* 15 (2003) 353–389.
- [3] Y. Huang, X. Duan, Q. Wei, C.M. Lieber, *Science* 291 (2001) 630–633.
- [4] Y. Wu, H. Yan, M. Huang, B. Messer, J.H. Song, P. Yang, *Chem. Eur. J.* 8 (2002) 1261–1268.
- [5] D.S. King, R.M. Nix, *J. Catal.* 160 (1996) 76–83.
- [6] J. Zhong, A.H. Kitai, P. Mascher, W.J. Puff, *Electrochem. Soc.* 140 (1993) 3644–3649.
- [7] H. Cao, J.Y. Xu, D.Z. Zhang, S.-H. Chang, S.T. Ho, E.W. Seelig, X. Liu, R.P.H. Chang, *Phys. Rev. Lett.* 84 (2000) 5584–5587.
- [8] D.M. Bagnall, Y.F. Chen, Z. Zhu, T. Yao, S. Koyama, M.Y. Shen, T. Goto, *Appl. Phys. Lett.* 70 (1997) 2230–2232.
- [9] D.S. Ginley, C. Bright, *Mater. Res. Soc. Bull.* 25 (2000) 15–21.
- [10] G.S. Trivikrama Rao, D. Tarakrama Rao, *Sens. Actuators B* 55 (1999) 166–169.
- [11] G. Agarwal, R.F. Speyr, *J. Electrochem. Soc.* 145 (1998) 2920–2925.
- [12] M.H. Huang, S. Mao, H. Feick, H. Yan, Y. Wu, H. Kind, E. Weber, R. Russo, P. Yang, *Science* 292 (2001) 1897–1899.
- [13] J.-J. Wu, S.-C. Liu, *Adv. Mater.* 14 (2002) 215–218.
- [14] J.-J. Wu, S.-C. Liu, *J. Phys. Chem. B* 106 (2002) 9546–9551.
- [15] R. Liu, A.A. Vertegel, E.W. Bohannon, T.A. Sorenson, J.A. Switzer, *Chem. Mater.* 13 (2001) 508–512.
- [16] K. Govender, D.S. Boyle, P. O'Brien, D. Brinks, D. West, D. Coleman, *Adv. Mater.* 14 (2002) 1221–1224.
- [17] L. Vayssieres, *Adv. Mater.* 15 (2003) 464–466.
- [18] S. Yamabi, H. Imai, *J. Mater. Chem.* 12 (2002) 3773–3778.
- [19] L.E. Greene, M. Law, J. Goldberger, F. Kim, J.C. Johnson, Y. Zhang, R.J. Saykally, P. Yang, *Angew. Chem. Int. Ed.* 42 (2003) 3031–3034.
- [20] L. Vayssieres, K. Keis, S.-E. Lindquist, A. Hagfeldt, *J. Phys. Chem. B* 105 (2001) 3350–3352.
- [21] L. Vayssieres, K. Keis, A. Hagfeldt, S.-E. Lindquist, *Chem. Mater.* 13 (2001) 4395–4398.
- [22] D.S. Boyle, G.K. Ovender, P. O'Brien, *Chem. Comm.* (2002) 80–81.
- [23] O.M. Hyama, H. Kozuka, T. Yoko, *Thin Solid Films* 306 (1997) 78–85.
- [24] A.W. Adamson, A.P. Gast, *Physical Chemistry of Surfaces*, sixth ed, Wiley, New York, 1997, pp. 328–342.
- [25] B. Wessler, L.F.F. Ange, M.W. Ader, *J. Mater. Res.* 17 (2002) 1644–1650.
- [26] M.H. Huang, Y. Wu, H. Feick, N. Tran, E. Weber, P. Yang, *Adv. Mater.* 13 (2001) 113–116.
- [27] J. Zhang, L.D. Sun, Y.J. Lin, H.L. Su, C.S. Liao, C.H. Yan, *Chem. Mater.* 14 (2002) 4172–4177.
- [28] J. Zhang, L.D. Sun, H.Y. Pan, C.S. Liao, C.H. Yan, *New J. Chem.* 26 (2002) 33–34.
- [29] Y. Li, G.W. Meng, L.D. Zhang, *Appl. Phys. Lett.* 76 (2000) 2011–2013.
- [30] Y.C. Wang, I.C. Leu, M.H. Hon, *J. Mater. Chem.* 12 (2002) 2439–2444.
- [31] K. Vanheusden, W.L. Warren, C.H. Seager, D.R. Tallant, J.A. Voigt, B.E. Gnade, *J. Appl. Phys.* 79 (1996) 7983–7990.